Science Advances
AAAS

advances.sciencemag.org/cgi/content/full/6/31/eaba6505/DC1

Supplementary Materials for

Dorsoventral polarity directs cell responses to migration track geometries

Emily O. Wisniewski, Panagiotis Mistriotis*, Kaustav Bera, Robert A. Law, Jitao Zhang, Milos Nikolic, Michael Weiger, Maria Parlani, Soontorn Tuntithavornwat, Alexandros Afthinos, Runchen Zhao, Denis Wirtz, Petr Kalab, Giuliano Scarcelli, Peter Friedl, Konstantinos Konstantopoulos*

*Corresponding author. Email: konstant@jhu.edu (K.K.); pmistriotis@auburn.edu (P.M.)

Published 31 July 2020, *Sci. Adv.* **6**, eaba6505 (2020)
DOI: 10.1126/sciadv.aba6505

The PDF file includes:

Figs. S1 to S6
Legends for movies S1 to S4

Other Supplementary Material for this manuscript includes the following:

(available at advances.sciencemag.org/cgi/content/full/6/31/eaba6505/DC1)

Movies S1 to S4

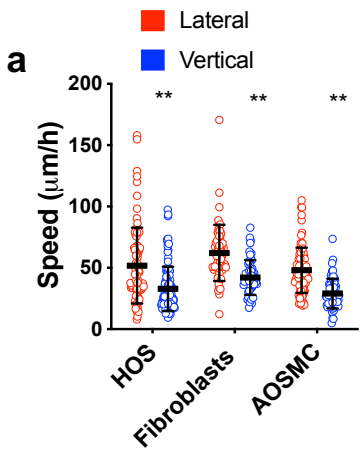

Supp. Figure 1. Both cancerous and non-cancerous cell lines migrate with different efficiencies in vertical versus lateral confinement. (a) Migration speeds of human osteosarcoma HOS cells (n≥84), dermal fibroblasts (n=58), and aortic smooth muscle cells (n≥66), from ≥3 independent experiments for each cell type. Data represent the mean±S.D.

** $p<0.01$ relative to lateral control.

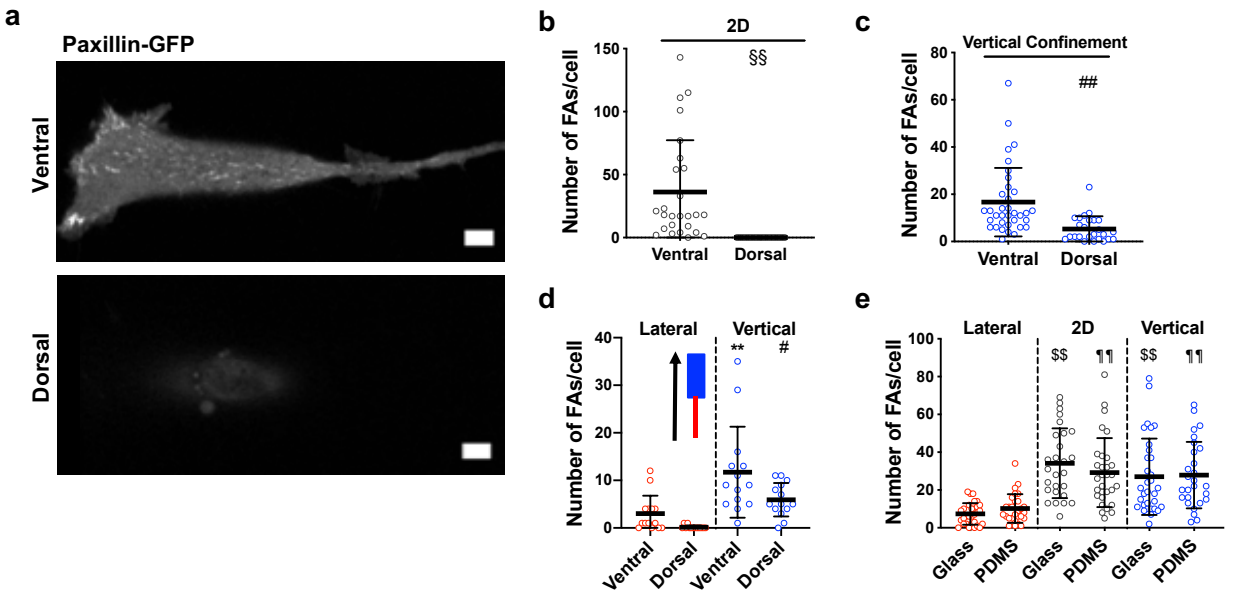

Supp. Figure 2. Focal adhesions are dorsoventrally polarized. (**a**) Representative images of a HT-1080 cell expressing paxillin-GFP on its ventral and dorsal surfaces on 2D. Scale bars: 5 µm. (**b-c**) Average number of paxillin-GFP-labelled focal adhesions on the dorsal and ventral surfaces of cells on 2D (n≥13 cells, 2 independent experiments) **(b)** or in vertical microchannels (n≥25 cells, 2 independent experiments) **(c)**. **(d)** Average number of paxillin-GFP-labelled focal adhesions on the ventral and dorsal surface of individual cells migrating through contiguous (lateral to vertical) channels (n=14 cells, 3 independent experiments). **(e)** Number of paxillin-GFP-labelled focal adhesions on 2D and inside lateral and vertical microchannels. The microchannel devices had either a glass or a PDMS basal surface (n≥28 cells, ≥3 independent experiments). Data represent the mean±S.D. §§ $p<0.01$ relative to 2D ventral; ** $p<0.01$ relative to lateral ventral; # $p<0.05$, ## $p<0.01$ relative to vertical ventral; $$ $p<0.01$ relative to lateral glass; ¶¶ $p<0.01$ relative to lateral PDMS.

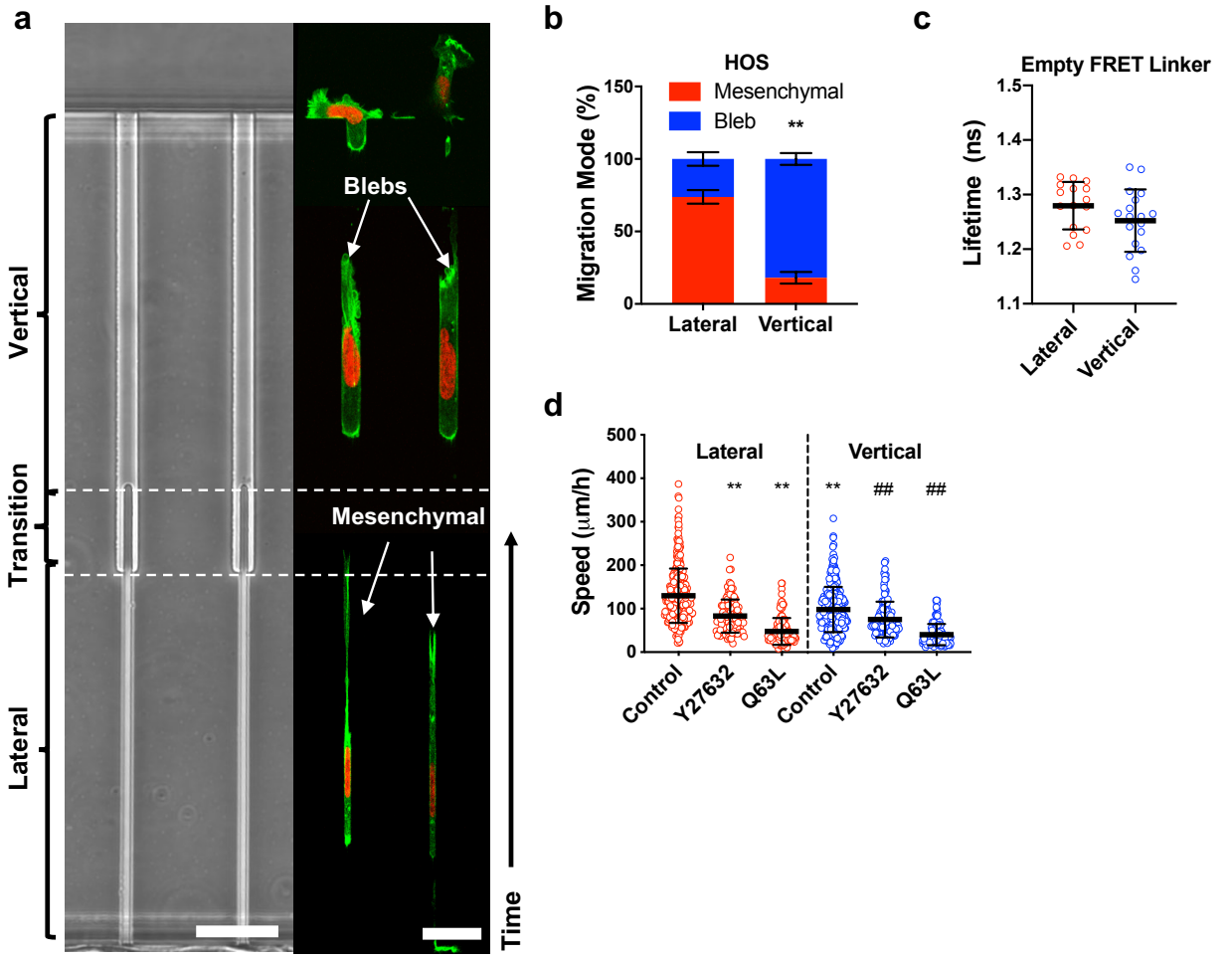

Supp. Figure 3. Confinement geometry regulates cell migration phenotype. (a) (Left) Phase contrast image of contiguous microchannels in which cells first experience lateral confinement before transitioning to vertical confinement. (Right) Representative images of the same mesenchymal LifeAct-GFP/H2B-mCherry-labelled HT-1080 cells in lateral confinement (bottom) transforming over time to a blebbing phenotype in vertical confinement (top). Scale bars: 40μm. **(b)** Percentage of HOS cells (n≥5 independent experiments, ≥20 cells per experiment) migrating with mesenchymal versus blebbing phenotypes in lateral and vertical confinement. **(c)** Lifetime of the empty FRET linker of cells migrating inside vertically or laterally confined channels (n≥16 cells, 2 independent experiments). **(d)** Migration speeds of HT-1080 cells, either controls, Y27632-treated (10 μM) or expressing constitutively active RhoA (Q63L), in confinement (n≥118 cells, ≥2 independent experiments). Values represent mean±S.D. **(c,d)** or mean±S.E.M **(b)**. ** $p<0.01$ relative to lateral control; ## $p<0.01$ relative to vertical control.

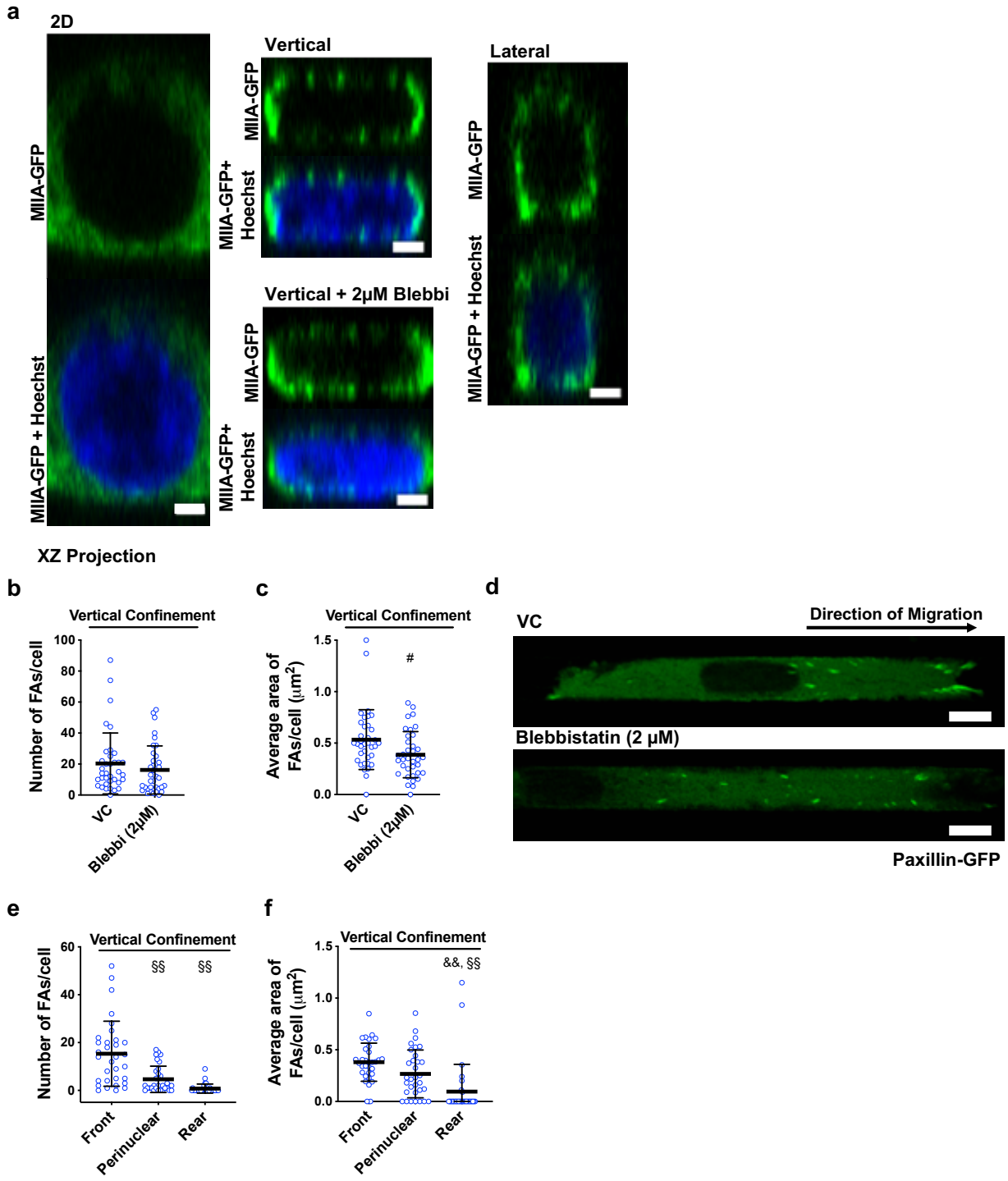

Supp. Figure 4. Perinuclear myosin regulates tension in confinement. (a) Images of perinuclear myosin (XZ plane projection) from representative HT-1080 cells expressing myosin-IIA-GFP and stained with Hoechst on 2D or in vertical (+/- 2 μm blebbistatin) or lateral confinement. Scale bars: 2 μm. **(b-c)** Average number **(b)** or area **(c)** of paxillin-GFP-labelled

focal adhesions of VC or blebbistatin (2 μM) treated HT-1080 cells in vertical microchannels (n=36 cells, 3 independent experiments). **(d)** Representative images of paxillin-GFP labelled focal adhesions of VC and blebbistatin (2 μM) treated cells in vertical channels. Scale bars: 10 μm. **(e-f)** Average number **(e)** or area **(f)** of paxillin-GFP-labelled focal adhesions in the front, perinuclear, and rear regions of vertically confined cells (n=32 cells, 3 independent experiments). # $p<0.05$ relative to vertical VC; §§ $p<0.01$ relative to vertical front; && $p<0.01$ relative to vertical perinuclear. Values represent mean±S.D.

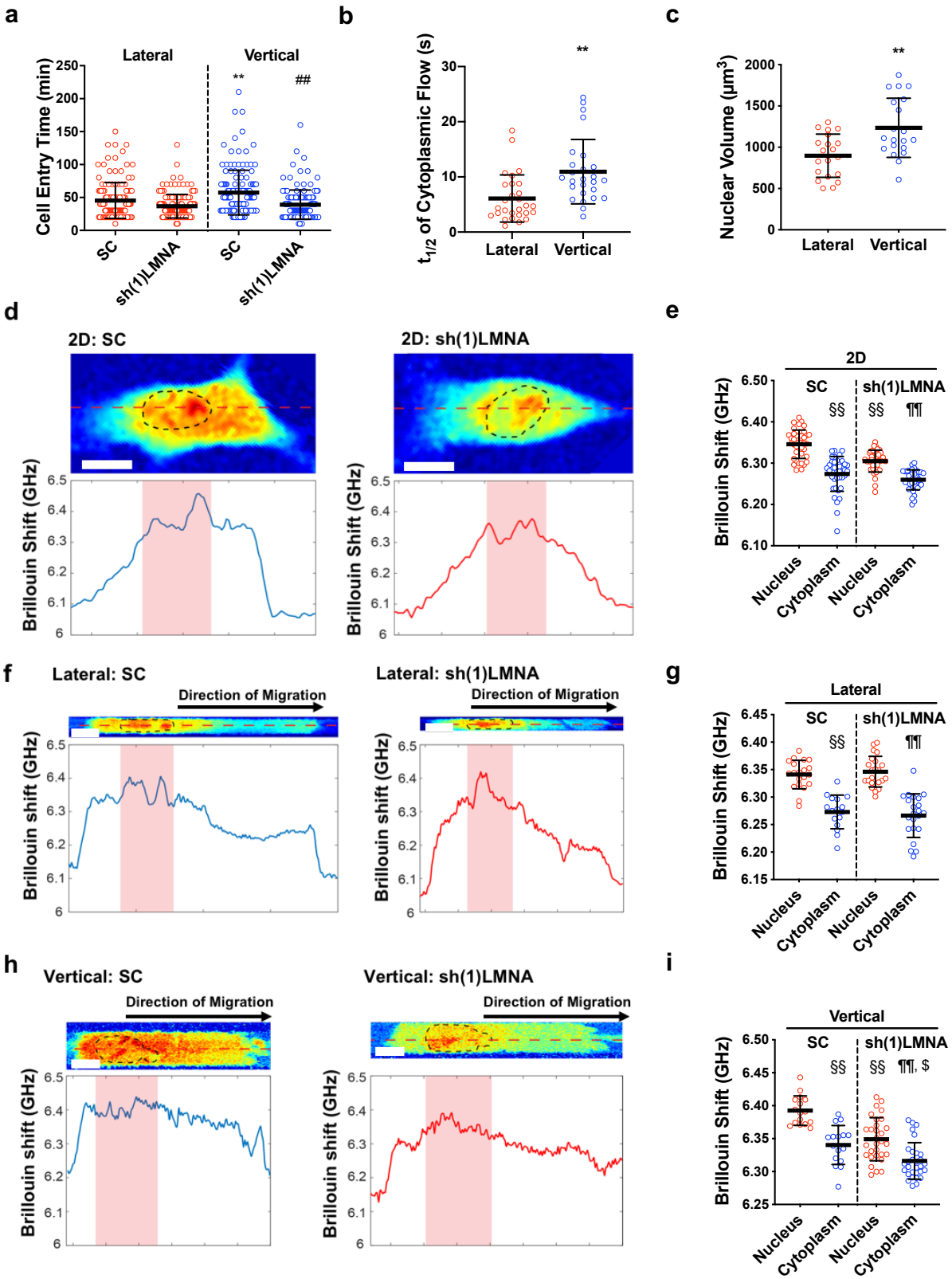
a
Lateral
Vertical
Cell Entry Time (min)
250
200
150
100
50
0
**
##
SC
sh(1)LMNA
SC
sh(1)LMNA
b
t1/2 of Cytoplasmic Flow (s)
30
20
10
0
**
Lateral
Vertical
c
Nuclear Volume (μm3)
2000
1500
1000
500
0
**
Lateral
Vertical
d
2D: SC
2D: sh(1)LMNA
Brillouin Shift (GHz)
6.5
6.4
6.3
6.2
6.1
6
e
2D
SC
sh(1)LMNA
§§
§§
¶¶
Brillouin Shift (GHz)
6.50
6.40
6.30
6.20
6.10
Nucleus
Cytoplasm
Nucleus
Cytoplasm
f
Lateral: SC
Lateral: sh(1)LMNA
Direction of Migration
Direction of Migration
Brillouin shift (GHz)
6.5
6.4
6.3
6.2
6.1
6
g
Lateral
SC
sh(1)LMNA
§§
¶¶
Brillouin Shift (GHz)
6.45
6.40
6.35
6.30
6.25
6.20
6.15
Nucleus
Cytoplasm
Nucleus
Cytoplasm
h
Vertical: SC
Vertical: sh(1)LMNA
Direction of Migration
Direction of Migration
Brillouin shift (GHz)
6.5
6.4
6.3
6.2
6.1
6
i
Vertical
SC
sh(1)LMNA
§§
§§
¶¶, $
Brillouin Shift (GHz)
6.50
6.45
6.40
6.35
6.30
6.25
Nucleus
Cytoplasm
Nucleus
Cytoplasm

Supp. Figure 5. The nucleus is more efficiently deformed in lateral confinement. (a) Cell entry time of H2B-mCherry-labeled LMNA-KD or scramble control HT-1080 cells (n≥143, 3 independent experiments) in lateral and vertical channels. **(b)** $t_{1/2}$ required for the signal (PA-GFP) to reach maximum intensity at the cell leading edge following UV illumination at the cell trailing edge in laterally versus vertically confined cells (n≥26 cells, 3 independent experiments) **(c)** Nuclear volumes of cells in lateral and vertical channels, as measured from confocal Z-stacks of H2B-mCherry tagged HT-1080 cells (n=20 cells, 2 independent experiments). **(d, f, h)** Heat map (top) and Brillouin shift values along the indicated red line scan (bottom) from representative scramble (left) and lamin-A depleted (right) cells on **(d)** 2D, in **(f)** lateral and **(h)** vertical confinement. Red shading on line scan plots represents the nuclear region. **(e, g, i)** Brillouin shift values of the nucleus or cytoplasm for scramble control or LMNA KD cells on **(e)** 2D (n≥37 cells, ≥2 independent experiments), in **(g)** lateral (n≥16 cells, ≥2 independent experiments) and **(i)** vertical (n≥16 cells, ≥2 independent experiments) confinement. Values represent mean±S.D.
** $p<0.01$ relative to lateral control, ## $p<0.01$ relative to vertical control; §§ $p<0.01$ relative to scramble nucleus; ¶¶ $p<0.01$ relative to sh(1)LMNA nucleus; $ $p<0.05$ relative to scramble cytoplasm.

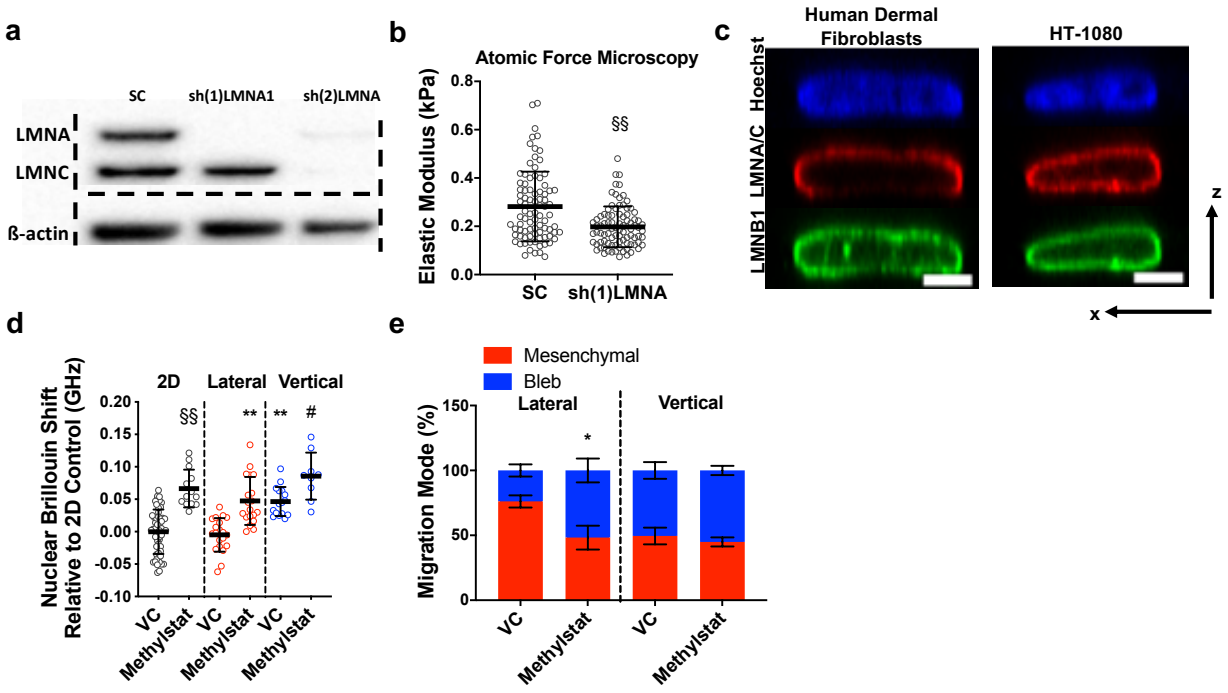

Supp. Figure 6. The nucleus is a mechanical barrier in vertical confinement. **(a)** Western blot showing LMNA/C knockdown efficiency. β-Actin was used as loading control. **(b)** Elastic modulus of the nucleus of SC and sh(1)LMNA cells, as quantified by fluorescent atomic force microscopy using H2B-mCherry-labeled cells pre-treated with LatA (2 μM) (n≥87 cells, 3 independent experiments). **(c)** XZ projections of representative nuclei of human dermal fibroblasts (left) or HT-1080 fibrosarcoma cells (right) on 2D stained for *lamin-A/C* and *lamin-B1*. **(d)** Nuclear Brillouin shift relative to 2D control values for VC and methylstat-treated HT-1080 cells in 2D, lateral, and vertical confinement (n≥9 cells, ≥2 independent experiments) In this experiment, values were normalized to 2D control nuclear Brillouin shift values to account for differences in calibration of the instrument over multiple days of experimentation. **(e)** Migration phenotypes of VC and methylstat-treated HT-1080 cells (n≥2 independent experiments, ≥10 cells per condition). Values represent mean±S.D. **(b,d)** or mean±S.E.M. **(e)**. Scale bars: 5 μm. * p<0.05, ** p<0.01 relative to lateral control, #p<0.05 relative to vertical control, §§ p<0.01 relative to 2D control.

Video Legends

Suppl. Video 1. Migration of cells in lateral and vertical channels. Representative HT-1080 cells migrate through laterally (10μm H x 3μm W) and vertically (10μm W x 3μm H) confined channels. Scale bar represents 50 μm.

Suppl. Video 2. Migration through contiguous lateral/vertical channels. HT-1080 cells migrate through contiguous microchannels, transitioning from lateral to vertical orientation (left) or vertical to lateral orientation (right). Scale bar represents 40 μm.

Suppl. Video 3. Myosin II inhibition prevents efficient rear end retraction during cell migration. HT-1080 cell expressing LifeAct-GFP and H2B-mCherry treated with 50μM Blebbistatin migrating in laterally confined microchannel. Scale bar represents 10 μm.

Suppl. Video 4. Treatment with low doses of blebbistatin does not inhibit rear end retraction during cell migration. HT-1080 cell expressing LifeAct-GFP and H2B-mCherry treated with 2μM blebbistatin migrating in laterally confined microchannel. Scale bar represents 10 μm.